Session 26*

* You are not responsible for the material in this lecture on the Final Exam.

Biologically Inspired Nonlinear Processing of Radar Waveforms

Shahzada Rasool and Mark R. Bell
School of Electrical and Computer Engineering
Purdue University

Other Approaches to Waveform Processing

- Matched-filtering has the goal of maximizing SNR, not optimizing delay-Doppler resolution.
- Echo-locating bats appear to possess spatial resolution characteristics superior to that dictated by the ambiguity function of their transmitted waveform.
- This suggests they are doing something other than matched-filtering:
- Neurological studies of echolocating bats indicate that thye perform a form of nonlinear correlation of the received signal with the transmitted signal.
- Neurological studies indicate that different temporal parts of the waveform are processed in different parts of the brain—they are processed separately and combined.

Other Approaches to Waveform Processing

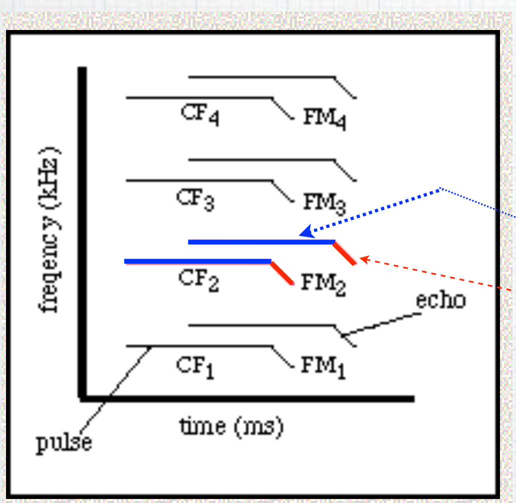

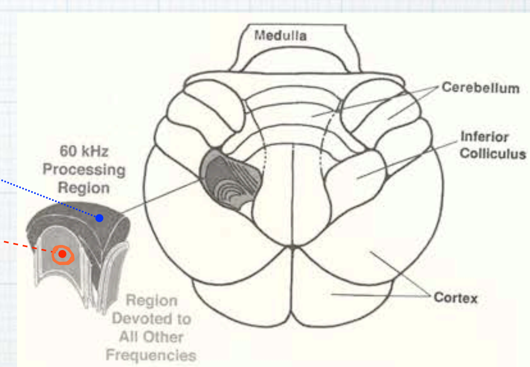

- This suggests that the bat processes different parts of the waveform separately and then combines the results using some form of (nonlinear) neural processing.
- Perhaps mimicking this separated processing structure would yield useful results in terms of delay-Doppler resolution enhancement or ambiguity reduction.

The V-Chirp Waveform

The *V-chirp signal* is made up of two successive chirps: an up-chirp with chirp-rate k_1 and a down-chirp with chirp rate k_2.

$$s(t) = s_1(t) + s_2(t - T),$$

where

$$s_1(t) = e^{j\pi k_1 t^2} \cdot 1_{[0,T]}(t) \quad \text{and} \quad s_2(t) = e^{j\pi k_2 (t-T)^2} \cdot 1_{[0,T]}(t)$$

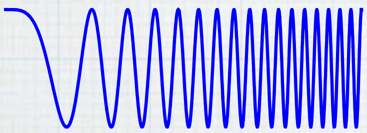

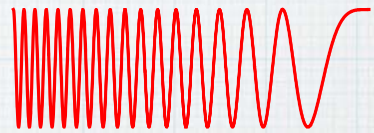

$$s(t) = s_1(t) + s_2(t - T)$$

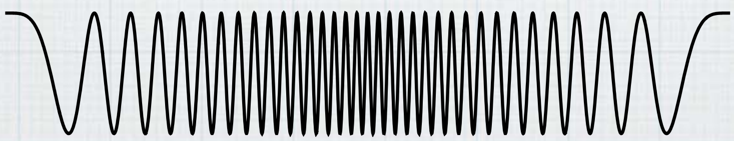

Approaches to Processing a V-Chirp

Matched-Filter Processing

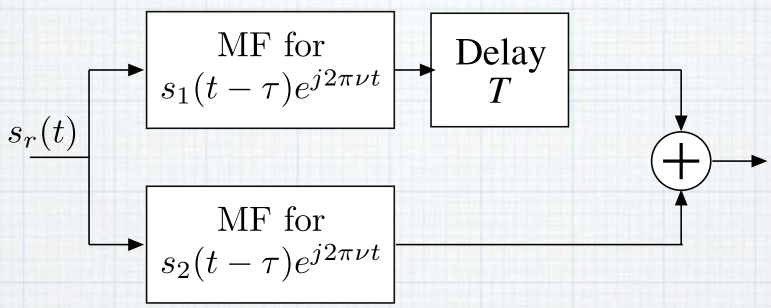

Matched-Filter Bank Processing

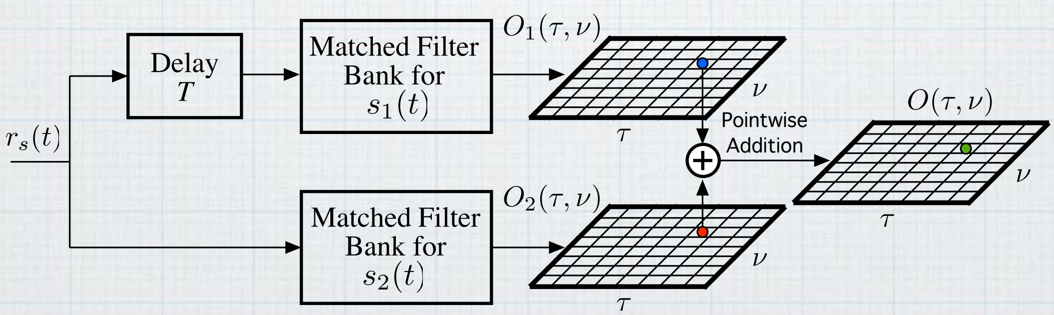

Ambiguity Function of an V-Chirp with k_1 = 33 and k_2 = 66

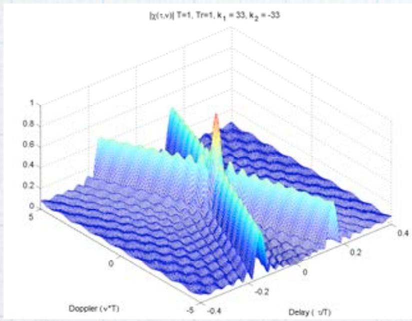

(a) Normalized ambiguity surface for $k_1 = k_2 = 33, T_r = T$.

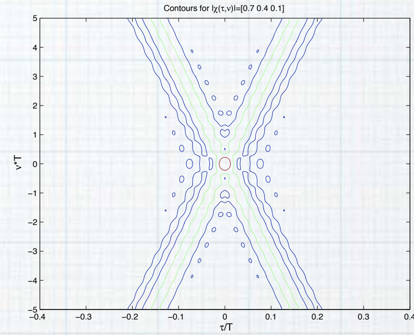

(b) Footprint of ambiguity surface for $k_1 = k_2 = 33, T_r = T$.

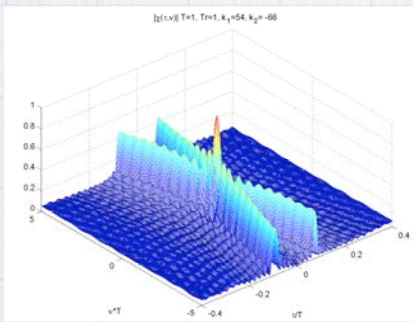

(c) Normalized ambiguity surface for $k_1 = 54, k_2 = 66, T_r = T$.

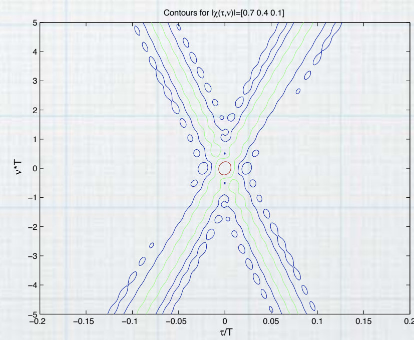

(d) Footprint of ambiguity surface for $k_1 = 54, k_2 = 66, T_r = T$.

Figure 2: Normalized ambiguity surfaces for different sweep rates.

Approaches to Processing a V-Chirp

Matched-Segment Pointwise Nonlinear Processing

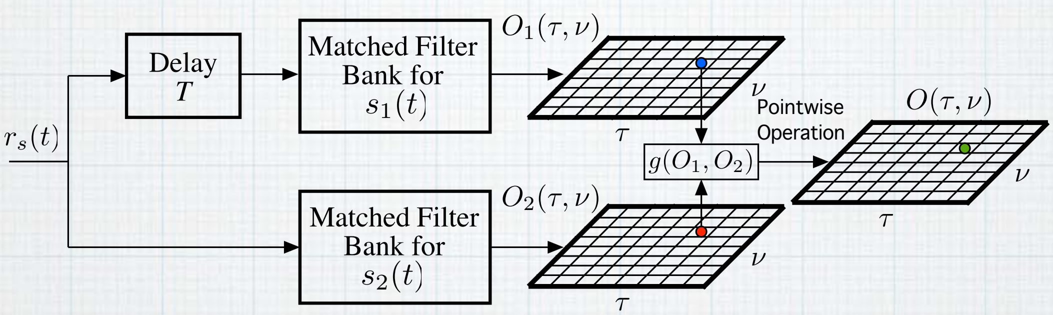

Matched-Segment Global Nonlinear Processing

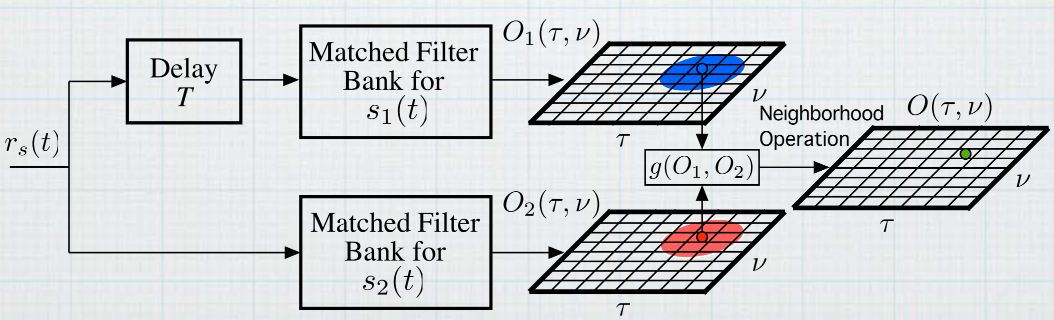

Approaches to Processing a V-Chirp

Matched-Segment Product Processing

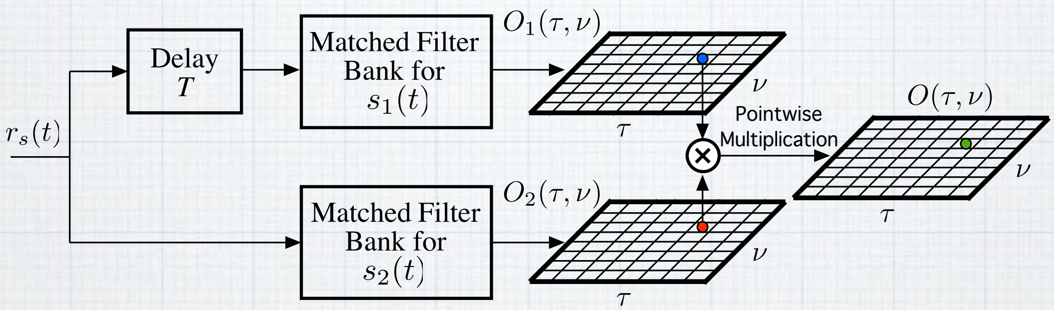

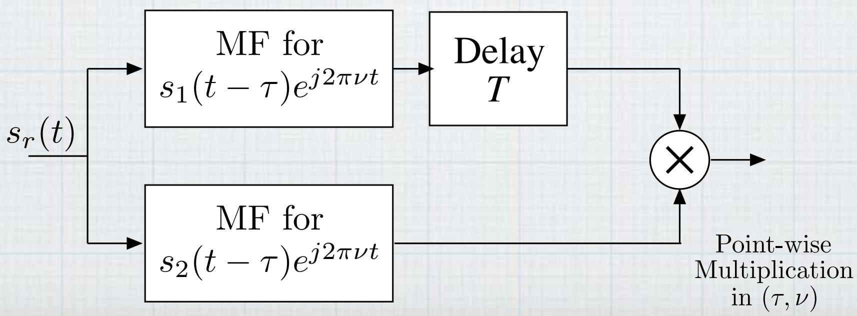

Delay-Doppler Response of Matched-Segment Product Processor

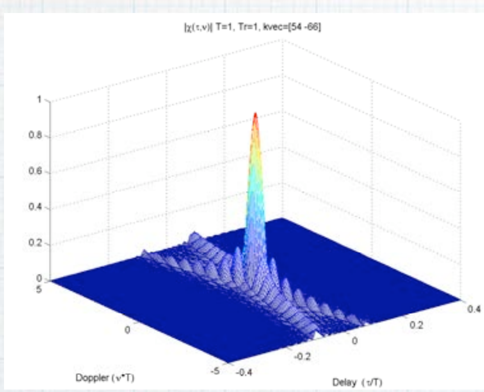

(a) Normalized Absolute Response

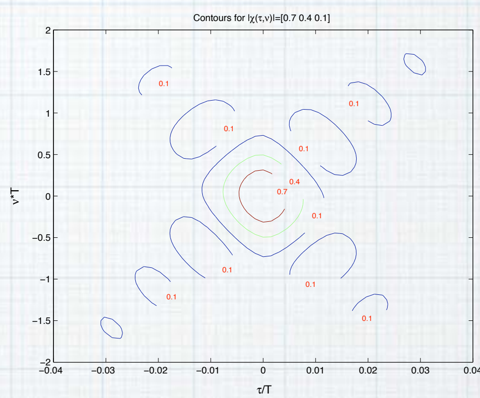

(b) Footprint

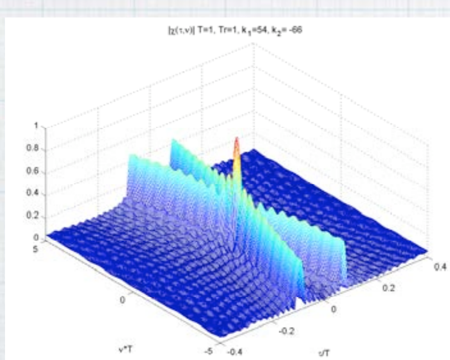

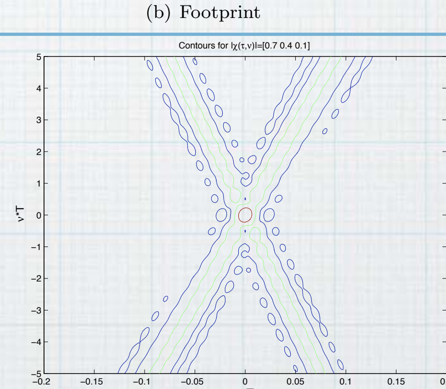

Matched-Filter bank Response for Purpose of Comparison

Two Targets: One at (0,0) and one at (0.02,1) [-10dB]

For V-chirp, $T = 1$, $T_{max} = 2$, $k_1 = 54$, $k_2 = -66$.

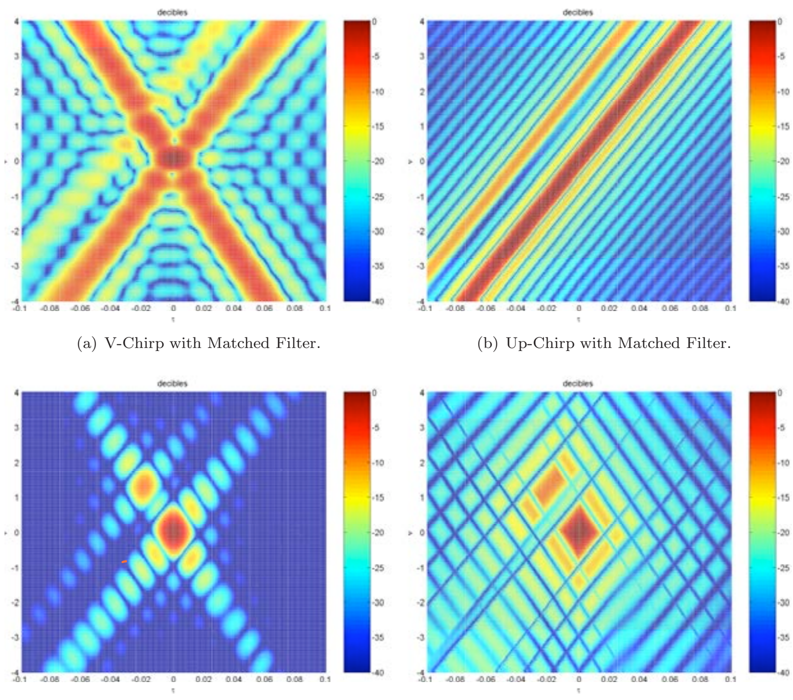

(a) V-Chirp with Matched Filter. (b) Up-Chirp with Matched Filter.

(c) Product Receiver with V-Chirp. (d) Minimum Receiver with V-Chirp.

Detection Performance

Consider a particular resolution cell (τ_0, ν_0) where we are testing for a target. Assume $(\tau_0, \nu_0) = (0, 0)$ WLOG:

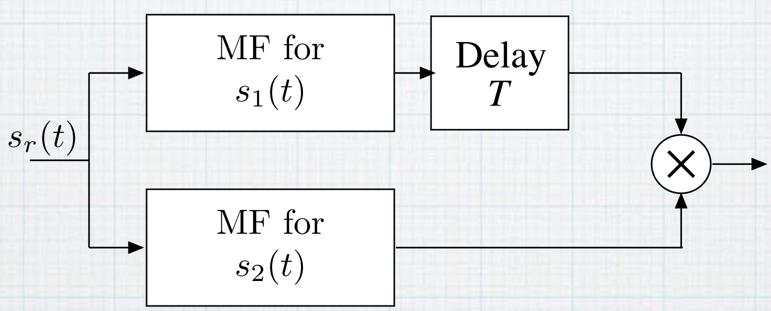

Let $s_1(t)$ and $s_2(t)$ be two orthogonal signals, each of duration T, and let

$$s(t) = s_1(t) + s_2(t - T).$$

Detection Performance (Continued)

Assuming that a slowly fluctuating point target is present, the received signal is

$$s_r(t) = \begin{cases} Bs(t-\tau)e^{j2\pi\nu t} + n(t), & \text{under } H_1, \\ n(t), & \text{under } H_0, \end{cases}$$

where B is a complex Gaussian random variable and $n(t)$ an independent zero-mean complex Gaussian white noise process with variance $\sigma_n^2 = N_0$ (each quadrature component is $N_0/2$). We let $E[|B|] = \sqrt{\pi/2}\,\sigma_b$ and $E[|B|^2] = 2\sigma_b^2$.

Using our proposed receiver structure, the received signal is correlated with $s_1(t)$ and $s_2(t)$ individually:

$$\mathcal{O}_1(\tau,\nu) = \int_{\mathbf{R}} s_r(t)s_1^*(t-\tau_0)e^{-j2\pi\nu_0 t}\,dt,$$

$$\mathcal{O}_2(\tau,\nu) = \int_{\mathbf{R}} s_r(t)s_2^*(t-\tau_0)e^{-j2\pi\nu_0 t}\,dt.$$

Detection Performance (Continued)

Without loss of generality, we can take $\tau_0 = \nu_0 = 0$. Then the output of the first correlator under H_1 is

$$\begin{aligned}\mathcal{O}_1(\tau,\nu) &= \int_{\mathbf{R}} \left[B(s_1(t-\tau)+s_2(t-\tau))e^{j2\pi\nu t} + n(t)\right]s_1^*(t)\,dt \\ &= B\left[\chi_{1,1}^*(\tau,-\nu) + \chi_{1,2}^*(\tau,-\nu)\right] + n_1.\end{aligned}$$

Similarly,

$$\mathcal{O}_2(\tau,\nu) = B\left[\chi_{2,2}^*(\tau,-\nu) + \chi_{2,1}^*(\tau,-\nu)\right] + n_2.$$

$$\chi_{jk}(\tau,\nu) = \int_{-\infty}^{\infty} s_j(t)\,s_k(t-\tau)\,e^{+i2\pi\nu t}\,dt.$$

Detection Performance (Continued)

For simplicity, let

$$R_1 \stackrel{\triangle}{=} \mathcal{O}_1(\tau, \nu)$$

and

$$R_2 \stackrel{\triangle}{=} \mathcal{O}_2(\tau, \nu).$$

When a target is present at the nominal delay and Doppler, we have $\tau = \nu = 0$. Since $\chi^*(0,0) = 1$, and by signal orthogonality $\chi^*_{1,2}(0,0) = 0$, we have

$$R_i = \begin{cases} B\left[\chi^*_{i,i}(\tau, -\nu)\right] + n_i, & : H_1, \\ n_i, & : H_0. \end{cases}$$

for $i = 1, 2$. Since B and $n_i, i = 1, 2$ are independent gaussian variates, therefore, R_1 and R_2 are complex normal random variables:

$$f_{R_i|H_1}(r_i) = \frac{1}{\pi(2\sigma_b^2 + N_0)} \exp\left[\frac{-r_i^* r_i}{2\sigma_b^2 + N_0}\right],$$
$$f_{R_i|H_0}(r_i) = \frac{1}{\pi N_0} \exp\left[\frac{-r_i^* r_i}{N_0}\right],$$

for $i = 1, 2$.

Detection Performance (Continued)

Under H_0, R_1 and R_2 are uncorrelated and thus independent. So $|R_1|$ and $|R_2|$ are independent Rayleigh RVs. Letting $Z = |R_1 R_2|$, we have

$$f_{Z|H_0}(z) = \frac{4z}{c_0^2} K_0(2z/c_0)$$

where

$$c_0 = N_0,$$

and $K_0(z)$ is zero order modified Bessel function of the second kind

Under H_1, $R_i \sim \mathcal{CN}(0, 2\sigma_b^2 + N_0)$ and the covariance between real (imaginary) components of R_1 and R_2 is σ_b^2, and cross components are independent. R_1 and R_2 are thus correlated Rayleigh RVs. Letting $c_1 = 2\sigma_b^2 + N_0$

$$f_{Z|H_1}(z) = \frac{4z}{c_0(2c_1 - c_0)} I_0\Big(\frac{2z(c_1 - c_0)}{c_0(2c_1 - c_0)}\Big) K_0\Big(\frac{2zc_1}{c_0(2c_1 - c_0)}\Big),$$

where

$I_0(x) =$ zero-order modified Bessel function of first kind.

Detection Performance (Continued)

The resulting likelihood ratio is

$$\mathbb{L}(z) = \frac{c_0}{2c_1 - c_0} I_0\Big(\frac{2z(c_1 - c_0)}{c_0(2c_1 - c_0)}\Big) \frac{K_0(\frac{2zc_1}{c_0(2c_1-c_0)})}{K_0(2z/c_0)} \underset{H_0}{\overset{H_1}{\gtrless}} \gamma.$$

Since I_0 and K_0 are monotone functions, an equivalent test is

$$Z \underset{H_0}{\overset{H_1}{\gtrless}} \gamma_c,$$

where γ_c is a function of c_0 and c_1 and is selected to achieve a specific false alarm probability.

Detection Performance (Continued)

Probability of false alarm:

$$\begin{aligned} P_{FA} &= \Pr[Z \geq \gamma_c | H_0] \\ &= \int_{\gamma_c}^{\infty} \frac{4z}{c_0^2} K_0(2z/c_0) dz \\ &= \frac{2\gamma_c \cdot K_1(2\gamma_c/c_0)}{c_0}, \end{aligned}$$

where $K_1(z)$ is 1st order modified Bessel function of second kind.

Probability of detection:

$$\begin{aligned} P_D = \Pr[Z \geq \gamma_c \,| H_1] &= \int_{\gamma_c}^{\infty} f_{Z|H_1}(z) dz \\ &= \frac{2z}{c_0(2c_1 - c_0)} \big[I_0(2\gamma_c\alpha)K_1(2\gamma_c\beta)c_1 \\ &\quad + I_1(2\gamma_c\alpha)K_0(2\gamma_c\beta)c_1 - I_1(2\gamma_c\alpha)K_0(2\gamma_c\beta)c_0\big] \end{aligned}$$

where $\alpha = \frac{(c_1 - c_0)}{c_0(2c_1 - c_0)}$ and $\beta = \frac{c_1}{c_0(2c_1 - c_0)}$.

Product Receiver versus Conventional Matched-Filter

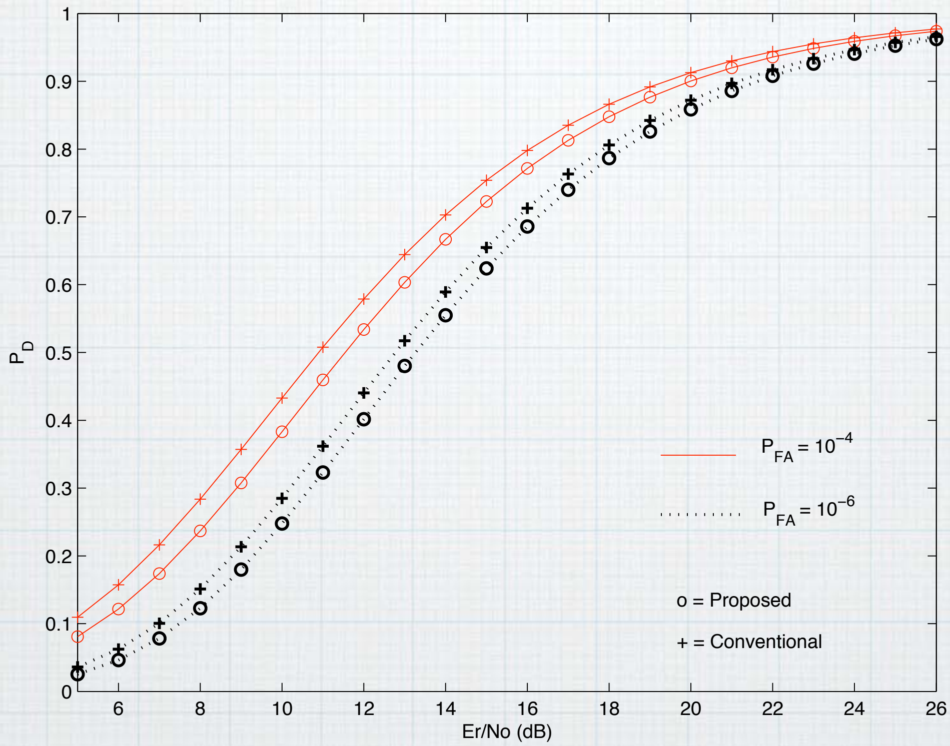

- Detection performance of proposed technique is close to optimal, especially at high SNR.
- Significant improvement in delay-Doppler resolution.

Matched-Segment Minimum Processor

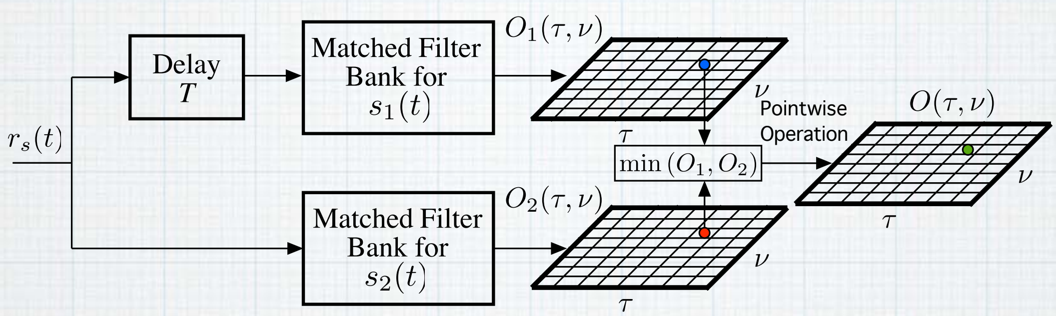

Minimum Receiver

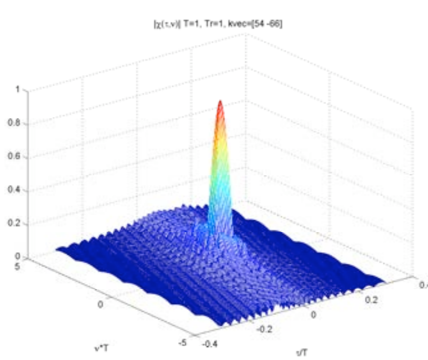

(a) Normalized Absolute Response

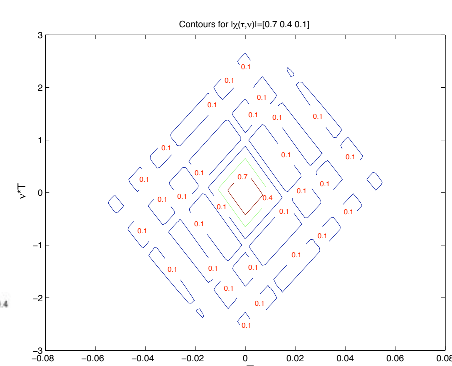

(b) Footprint

Two Targets: One at (0,0) and one at (0.02,1) [-10dB]

For V-chirp, $T = 1,\ T_{max} = 2,\ k_1 = 54,\ k_2 = -66.$

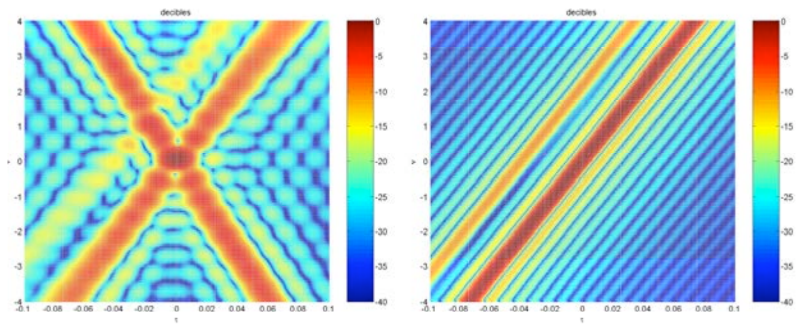

(a) V-Chirp with Matched Filter. (b) Up-Chirp with Matched Filter.

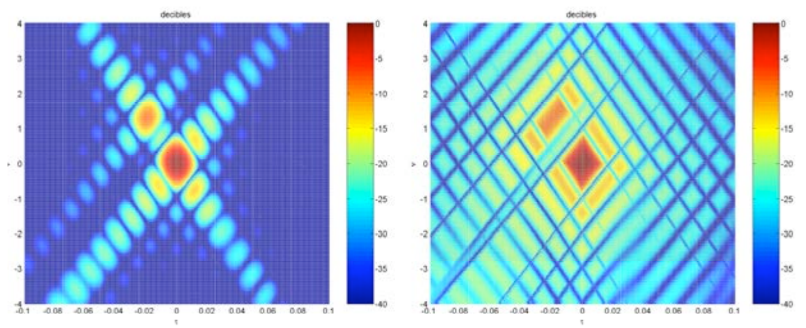

(c) Product Receiver with V-Chirp. (d) Minimum Receiver with V-Chirp.

Two Targets: At (0,0) and (0.08,0) [-15 dB]

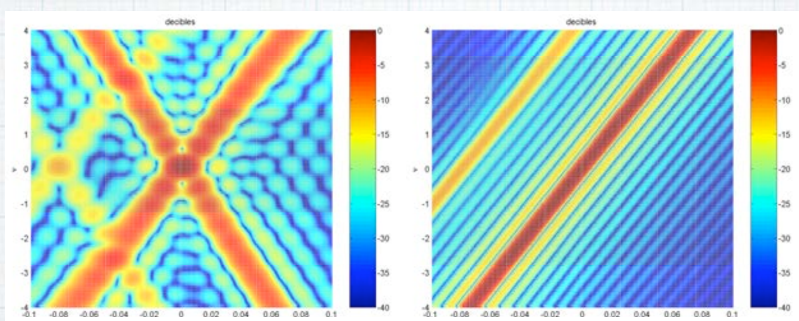

(a) V-Chirp with Matched Filter. (b) Up-Chirp with Matched Filter. $k = 54, T = 2$.

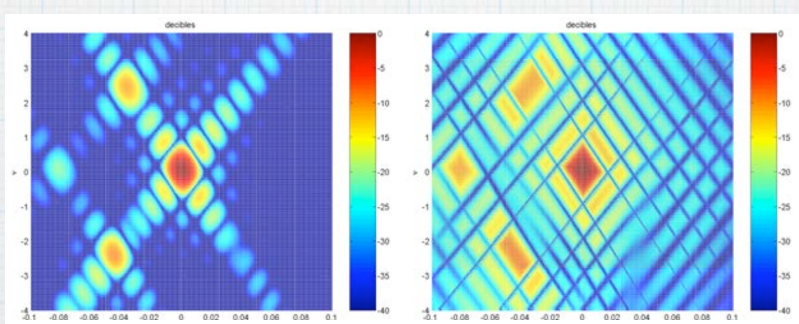

(c) Product Receiver with V-Chirp. (d) Minimum Receiver with V-Chirp.

Fig. 12. Response of different receivers for two targets 15 dB apart at $(0, 0)$ and $(0.08, 0)$. For V-chirp $T = 1$, $T_{max} = 2$, $k_1 = 54$, $k_2 = -66$.

Minimum Receiver versus Conventional Matched-Filter

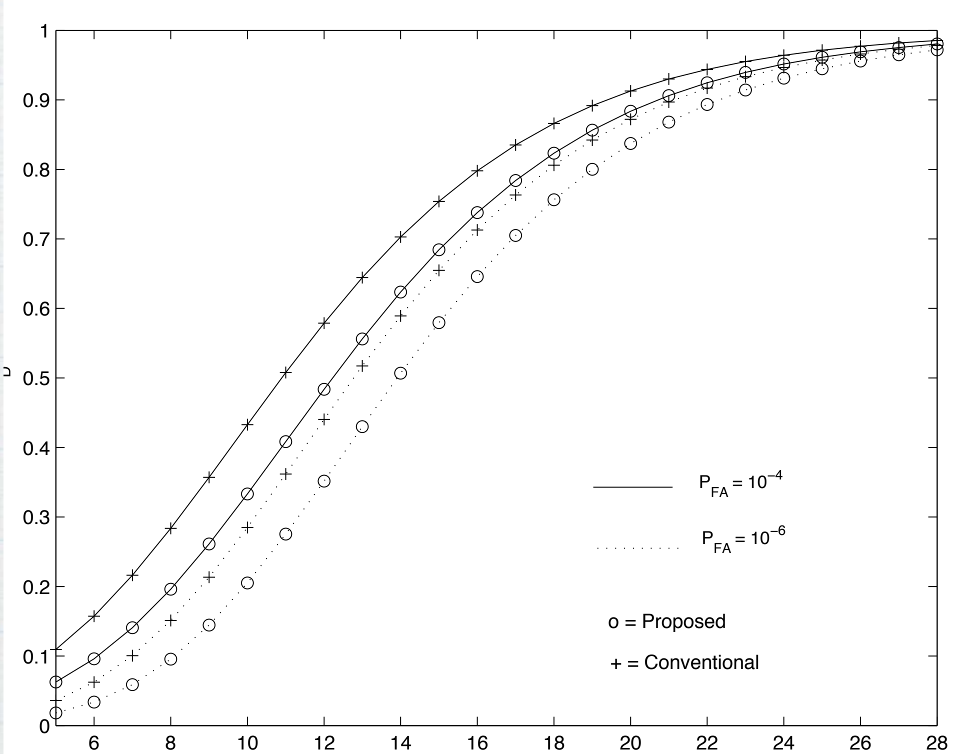

- Detection performance of proposed technique is close to optimal, especially at high SNR.
- Significant improvement in delay-Doppler resolution.

Comparison of Product and Minimum Receivers

Product Receiver:

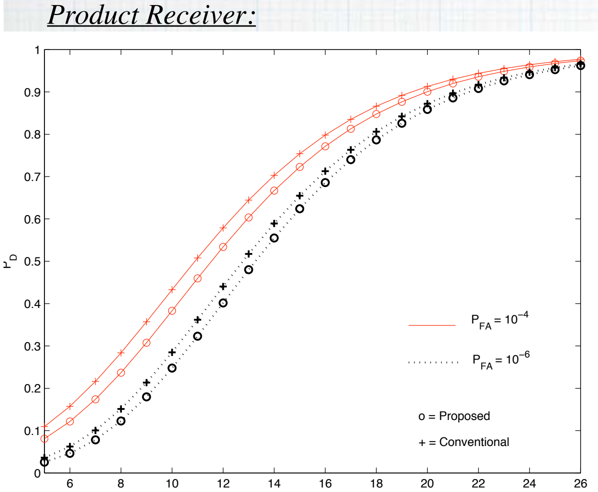

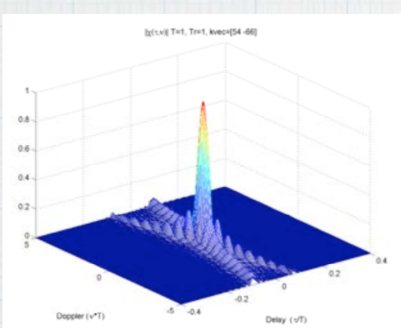

Minimum Receiver:

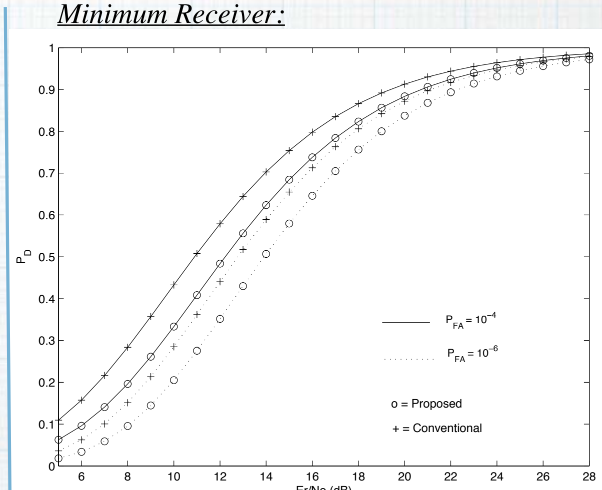

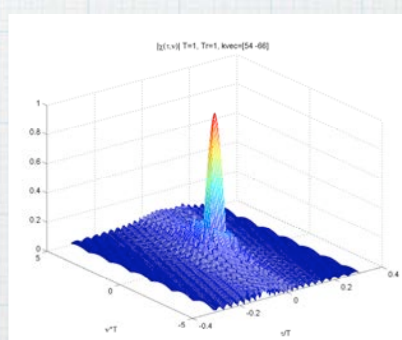

Future Work: Extension from Pointwise to Neighborhood Combining

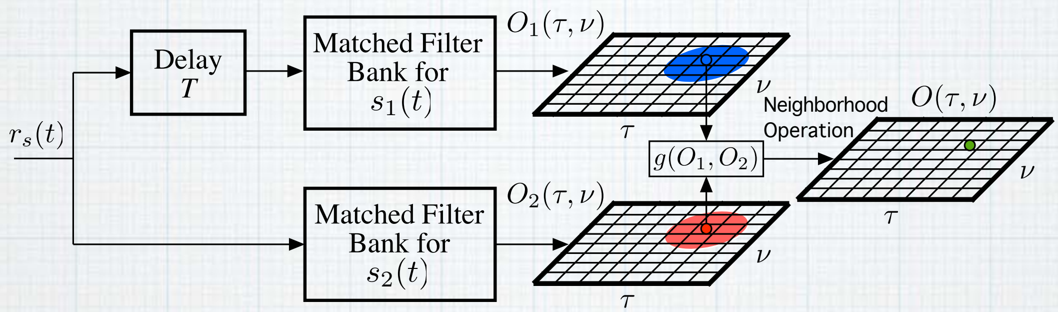

- There may be advantages to moving beyond pointwise nonlinear operations to nonlinear operations in a neighborhood about the delay-Doppler cell being processed

- Information about the modulus and phase of the segment ambiguity functions may be useful in formulating a neighborhood combining function.

- Example: Inhibition / Excitation models of cochlear and retinal processing.

- Closed-form detection performance may not be possible.

Future Work: Coded Waveform Segments

- Chirps are not the only waveforms that can be used with the *matched-segment processor.*

- We have investigated Costas waveforms. Moderately encouraging results, but further work needed.

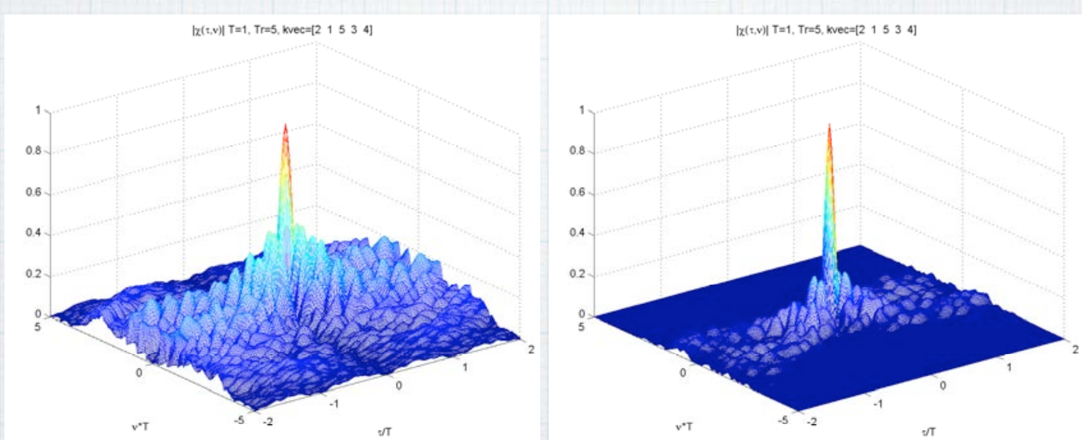

(a) Conventional receiver. (b) Proposed processing.

Fig. 13. Ambiguity surfaces for the Costas sequence of length 5.